10-24-2012

Fourier Transform Spectrometer (FTS) Servo Characterization and Improvement

M. Davidson

J. Elwell

J. Swasey

Fourier Transform Spectrometer (FTS) Servo Characterization and Improvement

M. Davidson, J. Elwell, J. Swasey,
Space Dynamics Laboratory, 1695 North Research Park Way, North Logan, Utah 84341

ABSTRACT

The high resolution and low measurement uncertainty goals for next generation atmospheric sounders will require FTS-based spectrometers which exhibit improved velocity stability and disturbance rejection over previous systems. This paper documents the characterization of and improvements made to existing SDL FTS systems as part of an internal study to meet the demands of future missions. Improved velocity tracking and disturbance rejection performance is documented along with selected lessons learned.

Keywords: Interferometer, Fourier Transform Spectrometer, Control System, Velocity Tracking, Velocity Stability, Servo, Disturbance Rejection

1. INTRODUCTION

The Space Dynamics Laboratory (SDL) has a long history of success with its Michelson Interferometer design as discussed in Robinson 2002, et al.[1] This includes cryogenic flight instruments operating down to liquid helium temperatures. Figure 1 shows the components of the Moving Mirror Carriage (MMC) of an SDL Fourier Transform Spectrometer (FTS).

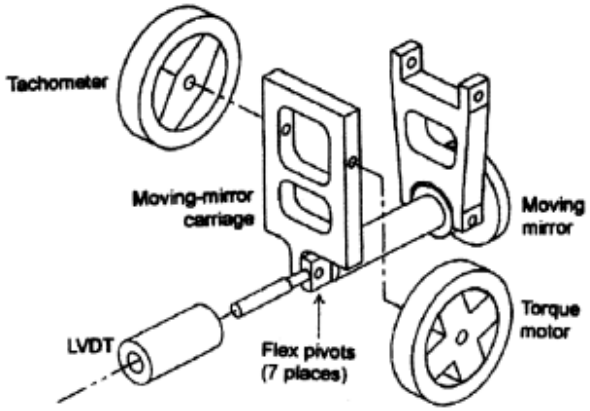

Figure 1 Translating mirror stage

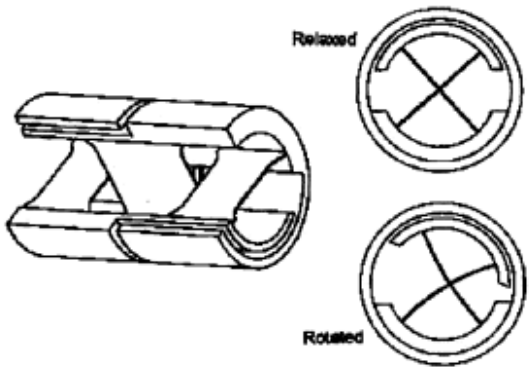

Figure 2 Flexural pivot

Figure 1. Components of a Moving Mirror Carriage (MMC)

A key element of this interferometer is the velocity control of the MMC, which requires very good velocity stability. The control system that executes this motion is commonly called the servo, and a block diagram of this system is shown in Figure 2. This block diagram shows the MMC, the control law, and the main source of feedback for this effort (which is not shown in Figure 1): velocity estimation using a laser interferometer channel realized in parallel with the science instrument.

Infrared Remote Sensing and Instrumentation XX, edited by Marija Strojnik, Gonzalo Paez,
Proc. of SPIE Vol. 8511, 851109 · © 2012 SPIE · CCC code: 0277-786X/12/$18 · doi: 10.1117/12.979862

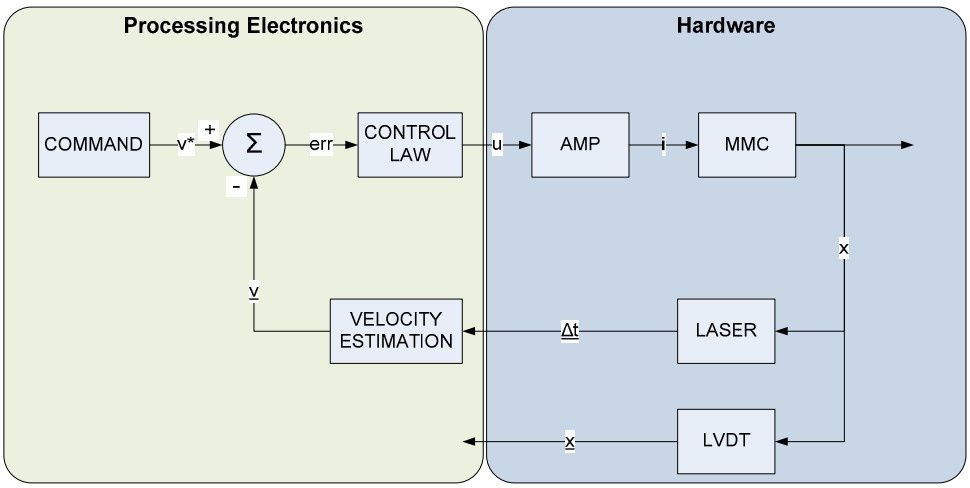

Figure 2. Servo System Signal Block Diagram

This paper documents major contributions to FTS servo performance in the areas of setpoint (command) tracking and disturbance rejection. Section 2 outlines groundwork done to characterize the MMC and laser velocity estimation elements using first principles modeling and system identification (System ID) techniques. Section 3 describes the hardware and algorithmic improvements made to the servo control law. Section 4 highlights some experimental results, focusing on the improved tracking and disturbance rejection performance. Section 5 summarizes our work and indicates research areas in which the next performance gains are likely to be found.

2. FTS SERVO CHARACTERIZATION

The following section focuses on characterization of the MMC, laser interferometer feedback and velocity estimation. The amplifier (AMP in Figure 2) is not discussed in this section. Sample results from System ID are presented at the end of the section, which provide validation of the first principles models.

2.1 Moving Mirror Carriage (MMC)

The MMC is the plant for the servo control system, with a position denoted as **x** in Figure 2. It is an underdamped mass-spring system, with a resonant peak due to the torsional stiffness of the flex pivots. For reference, see Figure 1, which shows the elements of the MMC.

The transfer function of the MMC *rotational* dynamics (neglecting the motor) is second order according to Elwell:[2]

$$\frac{\theta}{T_m} = \frac{\frac{1}{J}}{s^2 + \frac{B}{J}s + \frac{K}{J}} \tag{1}$$

where,

θ = MMC rotation angle

T_m = Torque applied by the motor

J = Moment of inertia of the MMC

B = Combined damping coefficient of flex pivots

K = Combined spring constant of flex pivots

For small angles, the relationship of position to rotation is $\mathbf{x=r\theta}$, where r is the moment arm of the MMC. In reality $x=r\sin(\theta)$, but the small angle approximation holds well enough for this effort.

The motor in the interferometer typically operates at very low speeds. Back-emf is negligible, and therefore the relationship between motor torque and applied current is

$$T_m = \frac{K_t}{R} \mathrm{i}$$

where,

Kt = Motor torque constant

R = Motor armature winding resistance

Collecting all these relationships gives the MMC transfer function (now including motor effects) from applied current to mirror *translation*:

$$\frac{x}{i} = \frac{\frac{rK_t}{RJ}}{s^2 + \frac{B}{J}s + \frac{K}{J}} \tag{1a}$$

This is the physical plant to be controlled.

2.2 Laser Interferometer Feedback

The laser channel of the interferometer is the main source of feedback for this effort. As such, a significant effort was made to understand and improve this sensor.

2.2.1 Transducer

The purpose of the servo control loop is to control the *velocity* of the translating mirror, but the laser channel of the interferometer (our feedback transducer) provides *position*. This requires us to numerically differentiate the position signal. There are countless ways to do this, and several were investigated in this study. The next section describes one of several velocity estimation algorithms investigated.

2.2.2 Fixed-Position Velocity Estimation

In the past, mirror velocity in the FTS was typically calculated from the laser feedback using what Brown et al[3] refer to as a "fixed-position velocity estimator". In this scheme of things, the velocity estimate is based on the measurement of time between the last two fringe crossings (**Δt** in Figure 3) during which the mirror traveled the known fixed distance **λ/2**. When a controller sample occurs, the estimate of mirror velocity used at time $\mathbf{t_k}$ is as follows:

$$v(t_k) = \frac{(\lambda/2)}{\Delta t} = \frac{\lambda}{2\Delta t} \tag{2}$$

This first-order derivative corresponds to the average velocity between the most recent laser fringe crossing and the one preceding it. A first-order backwards-difference velocity estimate like this introduces **Δt/2** latency into the estimate, as discussed in Carpenter et al.[4]

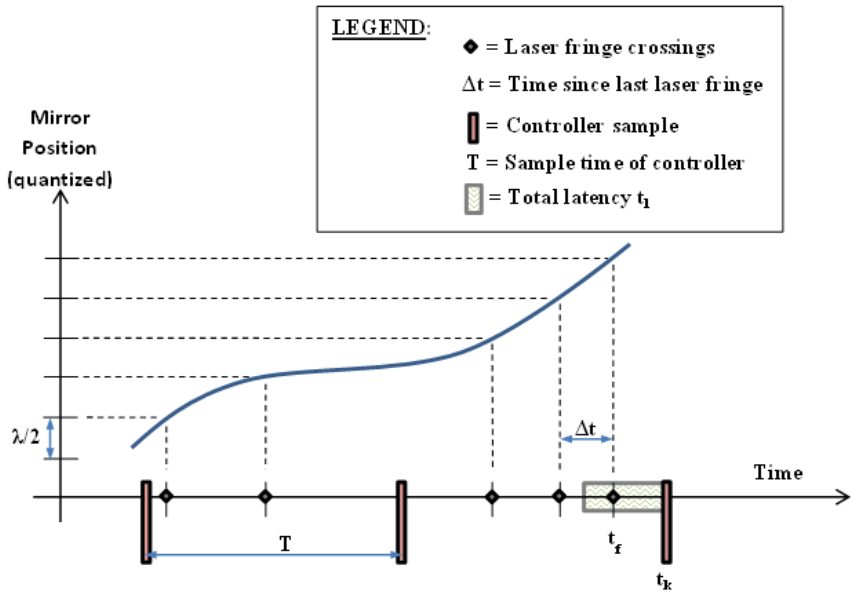

Figure 3. Velocity estimation quantities

In addition, this estimate of velocity was not valid at time t_k. Its time of validity is in the past, at time t_f, which is when the most recent fringe crossing actually occurred. It is clear from Figure 7 that this introduces an additional latency of $\mathbf{t_k - t_f}$ into our estimate of velocity using this method. The total latency inherent to the velocity estimation method of Equation 2 is then

$$t_l = \left(\frac{\Delta t}{2}\right) + \left(t_k - t_f\right) \tag{3}$$

This latency will cause phase loss, which degrades margins of stability in a controller. Note that the latency is velocity-dependent for a given laser wavelength. At very slow mirror speeds, where we have few or no laser fringe crossings during a sample time, either term of $\mathbf{t_l}$ could grow to be larger than the sample time **T**. At nominal speeds, where we have multiple fringes per controller sample time, the total latency must be a fraction of the sample time **T**.

At a constant mirror velocity **V**, we will see a fringe frequency of

$$f_f = \frac{V}{\left(\frac{\lambda}{2}\right)}$$

fringes per second. Counting these fringes at the high counter rate $\mathbf{f_{count}}$, we get

$$C = \frac{f_{count}}{f_f}$$

counts per fringe. We can resolve time within a quantization interval of

$$q_t = \frac{1}{C}$$

or one part in C. This means that at this nominal velocity **V**, our velocity measurement is quantized to a level of

$$q_v = q_t V = \frac{2V^2}{\lambda f_{count}} \tag{4}$$

Our velocity resolution is velocity-dependent, increasing with the square of velocity. If we had an infinite counter, we could resolve steady-state velocities approaching zero. The result of using a finite counter will be shown below.

Quantization noise is often assumed to be approximated by

$$\sigma_v{}^2 = \frac{q_v{}^2}{12}$$

from which the standard deviation of the noise due to velocity quantization can be found:

$$\sigma_v = \frac{2V^2}{\lambda f_{count}\sqrt{12}} \tag{5}$$

Our minimum resolvable velocity (due to saturation of the high rate counter) of

$$V_{min} = \frac{\left(\frac{\lambda}{2}\right)}{\Delta t_{max}} = \frac{\lambda f_{count}}{2S_{count}} \tag{6}$$

This deadband around zero velocity means we have a non-linear sensor. Our maximum resolvable velocity lies at the other end of the counter spectrum.

$$V_{max} = \frac{\left(\frac{\lambda}{2}\right)}{\left(\frac{1}{f_{count}}\right)} = \frac{\lambda f_{count}}{2} \tag{7}$$

The amplifier (not discussed here) and the physical plant (Equation 1a), coupled with the velocity estimate (Equation 2) comprise the plant to be controlled as shown in Figure 4.

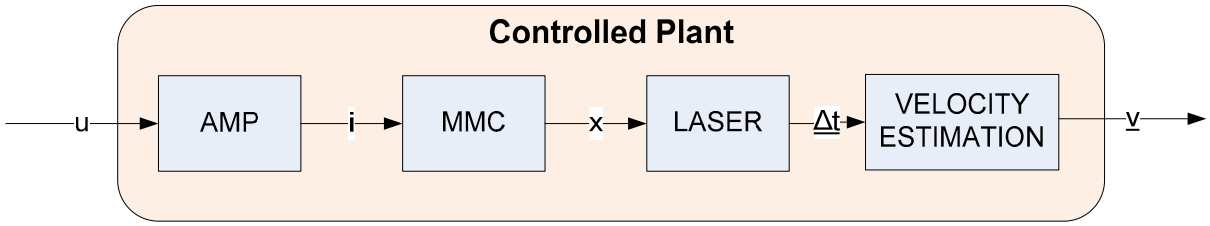

Figure 4. The controlled plant

2.3 System Identification (System ID)

System Identification is the method of exciting the plant with a known signal and measuring the response, in order to characterize the frequency response of the plant. The product of this process could be an input/output open-loop Bode plot or a transfer function that has been fit to the data. The System ID plant is then compared to the plant derived from first-principles as a check of the model. Many times, un-modeled dynamics are discovered during the System ID process, and these should be accommodated in the design of the control law. Simons et al[5] provide guidance on excitation signal selection and design.

For the purposes of System ID, the definition of the plant is broadened to include the sensors. The *controlled plant* is shown in Figure 4, and it includes the laser transducer as well as the velocity estimation method. Also included are sample-and-hold and calculation time effects.

Figure 5 shows the results of our final open-loop system IDs in a Bode plot format. The red curve represents the first principles model, and the blue curve represents the Bode plot obtained using system ID techniques. Previous system IDs had uncovered some un-modeled dynamics in the system, highlighting the need for hardware and software improvements. The system ID results, shown in Figure 5, were taken after these improvements were made. These results exhibit excellent model matching within the region of interest bounded by the range of the excitation frequency (~1-100Hz).

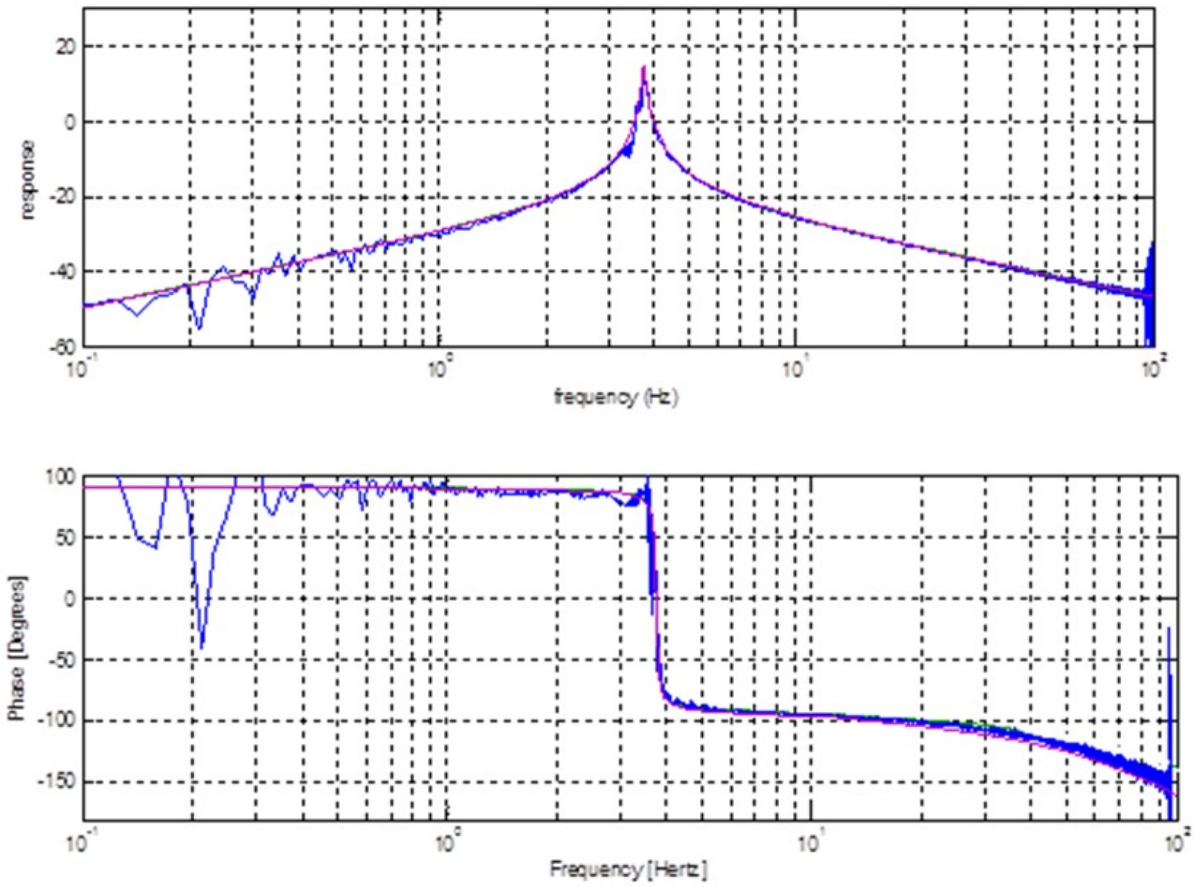

Figure 5. System ID compared with first principles

These results give confidence in taking the next step: improving the interferometer servo performance. There are no unexpected or un-modeled dynamics at play in this frequency range.

3. FTS SERVO IMPROVEMENTS

Our servo improvement approach concentrated on the following three areas:

- Improve the quality of velocity estimation
- Develop feedback control laws with enhanced bandwidth
- Develop advanced algorithms for disturbance rejection

The following subsections review our work in these three technology advancement areas.

3.1 Velocity Estimation Improvements

Several advanced velocity estimation techniques were developed during this study. All of these were simulated and only a subset were tested on the hardware. The simulation results indicate that several of these advanced estimation methods could significantly improve the quality of our velocity estimate. The results of our research on these topics are beyond the scope of this paper and will be presented elsewhere.

3.2 Improved Feedback Control Laws and Algorithms

A broad survey of candidate control laws and algorithms was conducted for this application. Twenty-eight control laws were narrowed down to the most likely five candidates, and sixteen assistive on-line control algorithms were narrowed down to the seven most likely candidates. Cost and schedule constraints prevented us from implementing all of these in hardware, but many were proven to perform well in simulation.

Of the two control laws, we had time to test on the FTS hardware, the front-runner was not surprisingly the ubiquitous PID controller.[6,7] Our model-based control design using the System ID plant to develop controller parameters paid off well, giving very good velocity stability and high bandwidth with our initial gains. Subsequent tuning only improved the servo performance. Results of our testing using the PID controller can be found in Section 4.

Although only four assistive on-line control algorithms were tested on interferometer hardware, all seven showed great potential in simulation. Of the four tested on the hardware, the two standouts were input shaping and a model-based disturbance rejection algorithm which we called Enhanced Control. Input shaping allowed for higher gains by keeping the system from reaching saturation. The Enhanced Control algorithm demonstrated our new ability to target specific monotonic disturbances (such as cryocooler harmonic vibrations) and effectively nullify their effect on mirror velocity. See Section 4 for more details.

4. EXPERIMENTAL RESULTS

This section presents some highlights from the results of hardware testing the candidate control laws and algorithms on a Michelson Interferometer.

4.1 PID Controller Results

The system generally matched simulation, although we were able to apply more gain than what we achieved in simulation before the onset of instability. This was perhaps due to a disparity between the simulated and the actual amplifier gain.

Figure 6 shows the drastically improved velocity stability of the updated FTS servo, using the PID controller. Bandwidth was significantly higher (~10x higher) than in previous servos, and therefore transient response and disturbance rejection were greatly improved with this updated servo control system design. Velocity response at turn-around (at the end of a mirror scan) was nearly critically-damped, notwithstanding the deadband around zero velocity described in Equation 6.

Our Enhanced Control successfully rejected the cryocooler fundamental vibration disturbance (reproduced using a loudspeaker with additional moving mass and confirmed with an accelerometer on the interferometer cube). This is shown in Figure 7. The FTS mirror no longer responds to the 53Hz fundamental of the crycooler, further improving velocity stability of the SDL interferometer. More than one monotonic disturbance can be rejected using this Enhanced Control algorithm at once.

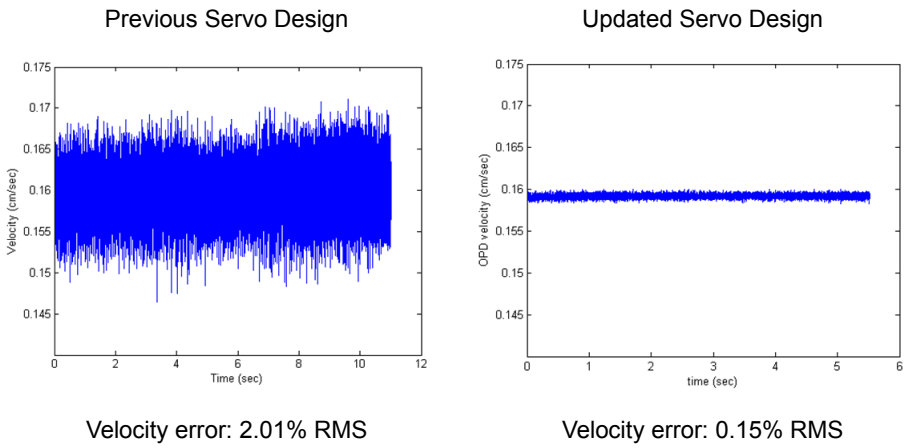

Figure 6. Velocity stability comparison of updated servo (using PID controller) to previous design

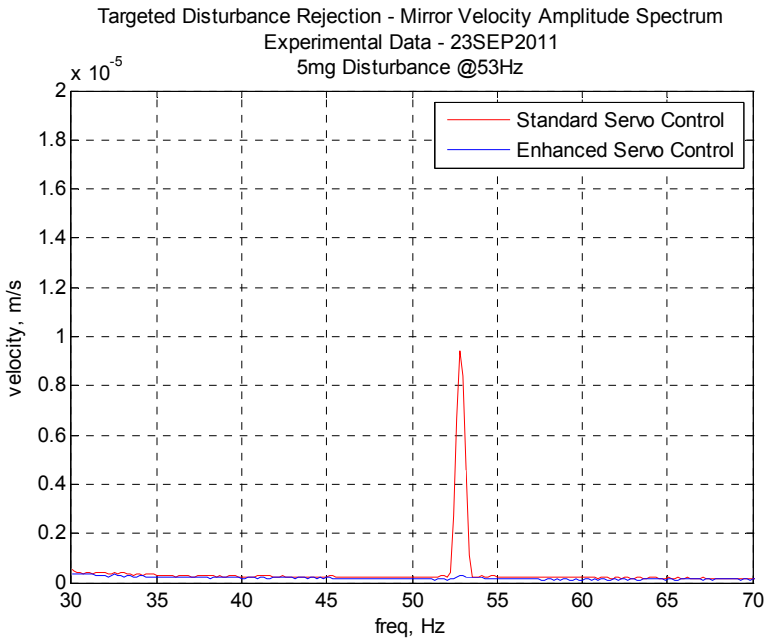

Figure 7. Experimental results of enhanced control rejecting monotonic vibration disturbance

5. CONCLUSIONS AND FUTURE WORK

The Space Dynamic Laboratory (SDL) continues to demonstrate its leading role in the development of Fourier Transform Spectrometers (FTS) by demonstrating an updated mirror control servo. This servo has significantly more bandwidth (~10x) and better velocity stability than its predecessors. The addition of Enhanced Control is an exciting development for future SDLs Michelson Interferometers, as this technology rejects monotonic disturbances from vibrations sources like crycoolers. The result of these improvements is an FTS servo with outstanding velocity stability which can meet the challenging demands of future science missions.

REFERENCES

[1] Robinson, R.C., Huppi, R.J., Folkman, S.L., "Optimization of a Cryogenic Mirror Stage," Proc. SPIE 4822, 72-81 (2002).
[2] Elwell, J., "A Digital Controller for a Michelson Interferometer," M.S. Thesis, Utah State University, Logan, Utah (1995).
[3] Brown, R. H., Schneider, S. C., and Mulligan M. G., "Analysis of Algorithms for Velocity Estimation from Discrete Position Versus Time Data," Proc. IEEE Transactions on Industrial Electronics, Vol 39, No. 1, FEB (1992).
[4] Carpenter, P., Brown, R., Heinen, J., Schneider, S., "On Algorithms for Velocity Estimation Using Discrete Position Encoders," Proc. IEEE IECON Conference on Industrial Electronics, Control, and Instrumentation, 844-849, Orlando, FL, (1995).
[5] Simons, G., Schoukens, J., "Robust Broadband Periodic Excitation Design," Proc. IEEE Transactions on Instrumentation and Measurement, Vol. 49, No. 2, April (2000).
[6] Santina, M., Stubberud, A., Hostetter, G., [Digital Control System Design 2nd ed.], Saunders College Publishing, (1994).
[7] Katsuhiko O., [Modern Control Engineering 3rd ed.], Prentice Hall, (1997).